

Analysis of Influencing Factors of Magnetic Characteristics of Permanent Magnet Bearings of Submersible Pumps for Wells

Xiaoguang Gao^{1,a,*}, Kaiyao Wei^{1,b}

¹School of Mechanical and Equipment Engineering, Hebei University of Engineering, Handan, Hebei, 056038, China

^a15356734246@163.com, ^bwky19970916@163.com

*Corresponding author

Abstract: In order to solve the problem of unbalanced force of traditional thrust bearings in the operation of well submersible pumps, a permanent magnet bearing device was designed. According to the magnetic features of two parallel rectangular section permanent magnets, a linear magnetic analysis model composed of rectangular section permanent magnet rings is proposed by using the imaginary displacement method and linear superposition principle. The influence of axial offset, axial length of a single ring and radial width of a magnetic ring on the magnetic characteristics of permanent magnet bearings was explored. The analysis results and simulation results show that the average deviation of the analytical computing value and the simulation result does not exceed 9.8%, which verifies that the analytical model is reasonable and accurate. And when the gap is fixed, the axial magnetic force first rises and then decreases with the growing of axial offset and the axial length of a single magnetic ring. It increases with the increase of the radial width of the magnetic ring. This research model provides technical support for the design computing of permanent magnet bearings and the optimization of structural parameters of submersible pumps for wells.

Keywords: Permanent Magnet Bearing; Magnetic Analysis Model; Axial Magnetic Force

1. Introduction

Well submersible pumps in the operation process will produce large axial force [1], and the existence of large axial force will inevitably affect the normal operation of the well submersible pump, the traditional method of well submersible pump axial force balance is to install thrust bearings on the pump shaft, by the thrust bearing to withstand the axial force [2]. The greater the axial force on the whole pump body, the greater the mechanical friction of the thrust bearing, thus increasing the wear of the thrust bearing, once the thrust bearing fails, the well submersible pump will have serious vibration and noise [3-5], and even cause damage to the submersible pump. Thrust bearing is a key part of the well submersible pump, to improve the service life of the well submersible pump must solve the constraints of the thrust bearing on its life.

Permanent magnetic bearings have a series of excellent characteristics such as microfriction, low power consumption, no pollution, high speed, no need for lubrication and sealing, and have a broad application prospect. In recent years, rare earth NdFeB permanent magnet materials have entered a period of high-speed development, domestic and foreign scholars have studied the mechanical properties of permanent magnet bearings, and the research methods mainly include equivalent magnetic charge method [6], molecular current method [7], vector magnetic potential method [8], virtual displacement method [9] and finite element method [10], etc. Delamare et al. [11] studied the configuration of permanent magnets in different magnetization directions, which laid a foundation for the research and design of permanent magnet bearings. In order to study the influence of non-uniform magnetization on the overall performance of repulsive permanent magnet bearings, Ohji [12-13] did a lot of finite element analysis and experiments, which had a great influence on the finite element analysis of permanent magnet bearings. Literature [14] studied the load carrying capacity of multiple pairs of concentric permanent magnet rings and analyzed the effects of magnetic cylinder remanent magnetization, cylinder gap radius, axial length and total magnetic circuit permeability on the magnetic force of permanent magnet bearings. Literature [15] studied the axial load carrying capacity of multiple double-ring concentric permanent magnet bearings, and the test showed that the sum of the magnetic

force of double-ring permanent magnet bearings composed of nested magnetic rings is much smaller than the axial magnetic force of multi-ring nested permanent magnet bearings. At this stage, most of the research stays in the bearing capacity of small permanent magnet bearings, in order to further develop the scope of application. In this paper, for the well submersible pump thrust bearing structure, according to the mechanical characteristics and structural features of the permanent magnet bearing, constructed a permanent magnet bearing magnetic force analytical model for high speed, large load bearing rotor, and verify the reasonableness of the analytical model through ANSYS finite element analysis software.

2. Structure and working principle

The structural section of the permanent magnet bearing is shown in Fig. 1, the thickness of the inner permanent magnet ring is b , the thickness of the outer permanent magnet ring is d , the axial length of the magnetic ring is a , and the radial air gap between the permanent magnet rings is h .

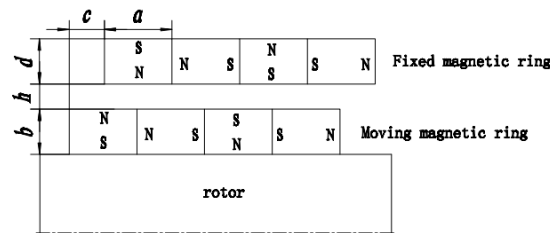


Figure 1: Structural diagram of permanent magnet bearing

In order to solve the problem of thrust bearing wear and rupture during the operation of well submersible pumps, this paper proposes the use of permanent magnet bearings to replace thrust bearings according to the specific working conditions of well submersible pumps. Using the above permanent magnet bearing structure, the permanent magnet bearing of the well submersible pump is designed. Fig.2 is the assembly diagram of the permanent magnet bearing of the well submersible pump. The fixed magnetic ring is fixed by the upper and lower outer ring, and the moving magnetic ring is slightly tampered in the direction of the rotating shaft, and the way of magnetization of the moving and fixed magnetic ring is shown in Fig.1. When the pump shaft is running at high speed, the pump shaft exerts pressure in the direction of the bearing, the permanent magnetic inner ring is offset with the rotating shaft, and according to the principle of magnetic poles, it generates magnetic force opposite to the axial force, so as to maintain the overall balance.

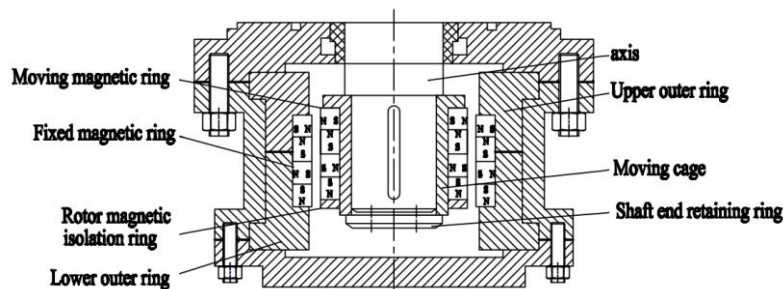


Figure 2: Schematic diagram of the assembly of permanent magnet bearings for submersible pumps for wells

3. Analytical model of axial force on rotor to be installed magnetic ring

Based on the magnetic characteristics of two parallel rectangular cross-section permanent magnets [16], the magnetic force analytical models of permanent magnet bearings with two different magnetization modes are constructed. Fig.3 and Fig.4 are the cross-section geometric parameters of permanent magnet bearings with reverse magnetization and rotating magnetization, respectively.

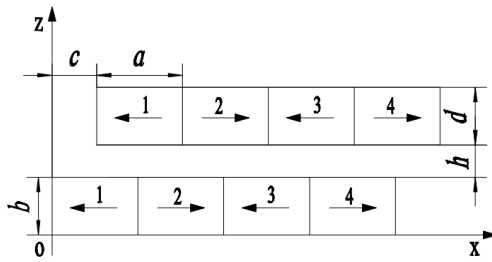


Figure 3: Section parameters of reverse magnetized permanent magnet bearing

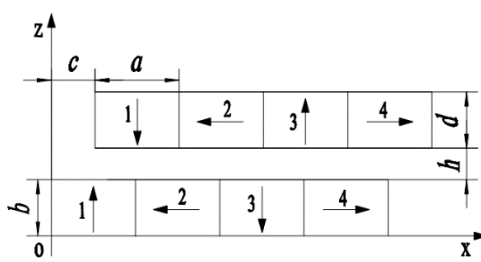


Figure 4: Section parameters of rotating magnetized permanent magnet bearing

The magnetic force analytical model of permanent magnet bearing is defined. F_{zkg} is the magnetic force of the k th inner magnetic ring to the g th outer magnetic ring in the z direction. F_{xkg} is the magnetic force of the k th inner magnetic ring to the g th outer magnetic ring in the x direction. The axial distance between the k th outer magnetic ring and the g th inner magnetic ring is $c_{kg} = c + (g - k)a$.

(1) For the reverse magnetized permanent magnet bearing, when $(k+g)$ is even, the magnetization mode of the inner magnetic ring and the outer magnetic ring is the same direction; when $(k+g)$ is odd, the magnetization mode of the inner magnetic ring and the outer magnetic ring is reverse. Based on the linear superposition principle, the total magnetic force of the reverse magnetized permanent magnet bearing in the z direction can be obtained as:

$$F_z = \sum_{k=1}^n \sum_{g=1}^n F_{zkg} = \sum_{k=1}^n \sum_{g=1}^n (-1)^{k+g+1} \frac{B_{r1} B_{r2} L \times 10^{-6}}{4\pi\mu_0} \phi(c_{kg}) \quad (1)$$

Similarly, the total magnetic force in the x -axis direction is:

$$F_x = \sum_{k=1}^n \sum_{g=1}^n F_{xkg} = \sum_{k=1}^n \sum_{g=1}^n (-1)^{k+g+1} \frac{B_{r1} B_{r2} L \times 10^{-6}}{4\pi\mu_0} \phi(c_{kg}) \quad (2)$$

(2) For the rotating magnetized permanent magnet bearing, according to the principle of linear superposition, F_z and F_x can be obtained as:

$$F_z = \frac{B_{r1} B_{r2} L \times 10^{-6}}{4\pi\mu_0} \left[\sum_{k=1}^n (n-k-1) \Phi(c_{k1}) + \sum_{g=2}^n (n-k-1) \Phi(c_{1k}) \right] \quad (3)$$

In the formula:

$$\Phi(c_{1g}) = \begin{cases} (-1)^m \phi(c_{1g}) & 1+g=2m(m=1,2,\dots) \\ (-1)^m \phi(c_{1g}) & 1+g=2m+1(m=1,2,\dots) \end{cases}$$

$$\Phi(c_{k1}) = \begin{cases} (-1)^m \phi(c_{k1}) & 1+k=2m(m=1,2,\dots) \\ (-1)^{m+1} \phi(c_{k1}) & 1+k=2m+1(m=1,2,\dots) \end{cases}$$

$$F_x = \frac{B_{r1} B_{r2} L \times 10^{-6}}{4\pi\mu_0} \left[\sum_{k=1}^n (n-k-1) \Theta(c_{k1}) + \sum_{g=2}^n (n-k-1) \Theta(c_{1g}) \right] \quad (4)$$

In the formula:

$$\Theta(c_{1g}) = \begin{cases} (-1)^m \phi(c_{1g}) & 1+g=2m(m=1,2,\dots) \\ (-1)^m \phi(c_{1g}) & 1+g=2m+1(m=1,2,\dots) \end{cases}$$

$$\Theta(c_{k1}) = \begin{cases} (-1)^m \phi(c_{k1}) & 1+k=2m(m=1,2,\dots) \\ (-1)^{m+1} \phi(c_{k1}) & 1+k=2m+1(m=1,2,\dots) \end{cases}$$

In the formula, h is the air gap width of the magnetic ring; c is the axial displacement of the magnetic ring; F_z is the bearing radial bearing capacity; F_x is the axial bearing capacity of the bearing; the magnetic unit is N; the length unit is mm.

4. Analytical model of axial force on rotor to be installed magnetic ring

The rare earth permanent magnet material used in this paper is NdFeB, and its performance is: $\beta_r = 1.13T$, $H_c = 800KA / m$, $\mu_r = \beta_r / \mu_0 H_c = 1.124$. Because the permanent magnet bearing is a rotating shaft stacked structure, the two-dimensional model can be used for finite element analysis. The geometric parameters of the permanent magnet bearing are set as follows: the inner radius of the moving magnetic ring is 15 mm, the outer radius of the moving magnetic ring is 20 mm, the inner radius of the fixed magnetic ring is 21 mm, the outer radius of the fixed magnetic ring is 26 mm, and the number of magnetic rings is 4.

4.1. Analysis of the influence of axial displacement of magnetic ring on magnetic force

The geometric parameters of the permanent magnet bearing are set: $b = d = 5mm$, $a = 5mm$, $h = 1mm$, and only the value of the axial displacement c of the magnetic ring is changed. The above parameters of the permanent magnet bearing are brought into Equation (2) to obtain the calculated value of the model, and compared with the simulation results. Table 1 is the calculation results of the reverse magnetization permanent magnet bearing model and the ANSYS simulation results. Fig.5 is the corresponding magnetic force curve. Through the chart, it can be concluded that when the axial displacement is between 0 and 2.5 mm, the axial magnetic force of the permanent magnet bearing shows a significant increase. When the axial displacement is between 2.5 ~ 5mm, the axial magnetic force of the permanent magnet bearing shows a sharp decrease trend, and the axial magnetic force reaches the maximum at 2.5mm.

Table 1: Calculated and simulated values of reverse magnetization axial magnetic force model

c/mm	0	0.5	1.0	1.5	2.0	2.5	3.0	3.5	4.0	4.5	5.0
F_{xj}/N	0	162.1	296.6	392.9	452.4	477.5	469.9	429.1	353.6	243.3	106.4
F_{xf}/N	0.62	172.3	263.6	348.2	399.4	419.4	412.3	370.6	309.5	225.6	92.7

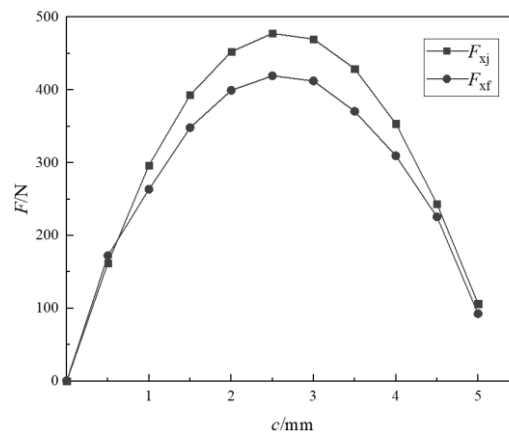


Figure 5: The change curve of calculated value and simulated value of reverse magnetization axial magnetic force

The geometric parameters of the permanent magnet bearing are set: $b = d = 5mm$, $a = 5mm$, $h = 1mm$, and only the value of the axial displacement c of the magnetic ring is changed. The above parameters of the permanent magnet bearing are brought into Equation (4) to obtain the calculated value of the model, and compared with the simulation results. Table 2 is the calculation results of the permanent magnet bearing model and the ANSYS simulation results, and Fig.6 is the corresponding magnetic force curve. It can be concluded from the chart that for the rotating magnetized permanent magnet bearing, when the axial displacement is between 0 ~ 5mm, the axial magnetic force of the permanent magnet bearing shows a significant increase trend. When the axial displacement is between 5 ~ 10mm, the axial magnetic force of the permanent magnet bearing shows a sharp decrease trend, and the axial magnetic force reaches the maximum at about 5mm. The maximum error between the calculation results of the model and the simulation results is 11.2 %, the minimum error is 1.6 %, and the average error is 8.6 %.

Table 2: Rotating magnetization axial magnetic force model calculation value and simulation value

c/mm	0	1	2	3	4	5	6	7	8	9	10
F_{xj} /N	0	212.8	439.2	590.7	682.6	687.5	586.3	440.7	282.6	115.6	-32.4
F_{xf} /N	-4.1	234.2	410.3	533.9	608.8	610.2	522.7	398.3	263.5	117.4	-35.5

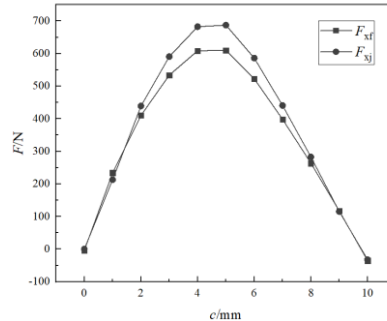


Figure 6: The variation curve of calculated value and simulated value of axial magnetic force of rotating magnetization

Fig.7 is the two-dimensional magnetic field line diagram of ANSYS simulation of rotating magnetized permanent magnet bearing. Through the comparative analysis of the above charts : when the number of magnetic rings is 4, the maximum bearing capacity of the reverse magnetized permanent magnet bearing is about 0.7 times the maximum bearing capacity of the rotating magnetized permanent magnet bearing.

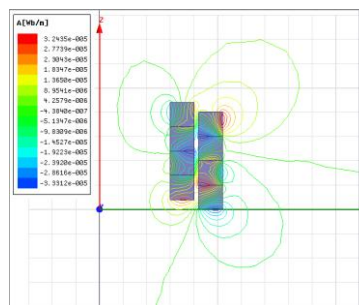


Figure 7: Rotary magnetized permanent magnet bearing ANSYS simulation of two-dimensional magnetic field line

4.2. Analysis of the influence of the axial length of the magnetic ring on the magnetic force

The geometric parameters of the permanent magnet bearing are set: $b = d = 5\text{mm}$, $h = 1\text{mm}$, $c = 1\text{mm}$, and only the axial length of the magnetic ring a is changed. The above parameters of the permanent magnet bearing are substituted into Formulas (2) and (4) to obtain the calculated values of the model, and compared with the simulation results. Table 3 is the calculation results of the permanent magnet bearing model and the ANSYS simulation results, and Fig.8 is the corresponding magnetic force curve. F_{xj} and F_{xf} represent the calculated value of the analytical model of reverse magnetization magnetic force and the simulation value of ANSYS software, respectively. F_{1xj} and F_{1xf} represent the calculated value of the analytical model of rotating magnetization magnetic force and the simulation value of ANSYS software, respectively. It can be concluded from the chart that for the reverse magnetized permanent magnet bearing, when the axial length of the magnetic ring is between 1mm and 8mm, the axial magnetic force of the permanent magnet bearing shows a sharp increase trend, and there is no maximum bearing capacity. For rotating magnetized permanent magnet bearings, when the axial length of the magnetic ring is between 1 ~ 4mm, the axial magnetic force of the permanent magnet bearing first increases significantly and then gradually becomes gentle. When the axial length of the magnetic ring is between 4 ~ 8mm, the axial magnetic force shows a slow decreasing trend, and the axial magnetic force reaches the maximum at about 4mm. The maximum error between the model calculation results and the simulation results is 17.4 %, the minimum error is 6.1 %, and the average error is 9.8 %.

Table 3: Comparison of model calculation value and simulation value Table 1

a/mm	1	2	3	4	5	6	7	8
F_{xj}/N	9.8	99.2	191.7	257.5	300.5	327.1	342.7	351.2
F_{xf}/N	8.9	80.6	169.4	224.3	267.8	282.3	308.6	330.1
F_{1xj}/N	30.1	156.1	207.7	218.6	217.8	201.4	189.1	177.6
F_{1xf}/N	48.5	183.4	227.9	238.2	234.2	225.2	203.3	188.4

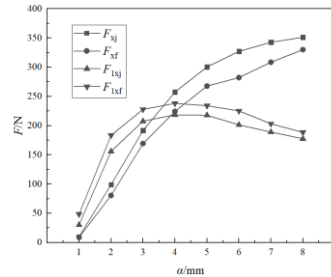


Figure 8: Curves of model calculation value and simulation value 1

4.3. Analysis of the influence of radial thickness of magnetic ring on magnetic force

The geometric parameters of the permanent magnet bearing are set as follows: $a = 5\text{mm}$, $h = 1\text{mm}$, $c = 1\text{mm}$, and only the radial thickness d ($d = b$) of the magnetic ring is changed. The above parameters of the permanent magnet bearing are substituted into Formulas (2) and (4) to obtain the calculated values of the model, and compared with the simulation results. Table 4 is the calculation results of the permanent magnet bearing model and the ANSYS simulation results, and Fig.9 is the corresponding magnetic force curve. F_{xj} and F_{xf} represent the calculated value of the analytical model of reverse magnetization magnetic force and the simulation value of ANSYS software, respectively. F_{1xj} and F_{1xf} represent the calculated value of the analytical model of rotating magnetization magnetic force and the simulation value of ANSYS software, respectively. It can be concluded from the chart that for the reverse magnetized permanent magnet bearing, when the radial thickness of the magnetic ring is between 1mm and 8mm, the axial magnetic force of the permanent magnet bearing shows a significant increase trend, and there is no maximum bearing capacity. For rotating magnetized permanent magnet bearings, when the thickness of the magnetic ring is between 1 ~ 8mm, the axial magnetic force of the permanent magnet bearing shows a significant increase trend, and there is no maximum bearing capacity. The maximum error between the model calculation results and the simulation results is 14.8 %, the minimum error is 1 %, and the average error is 7.3 %.

Table 4: Comparison of model calculation value and simulation value Table 2

d/mm	1	2	3	4	5	6	7	8
F_{xj}/N	58.3	138.3	204.8	256.1	296.6	329.7	358.6	384.1
F_{xf}/N	54.6	129.4	186.8	233.2	272.1	297.8	326.2	344.9
F_{1xj}/N	37.7	98.4	143.7	208.3	217.8	264.1	311.9	355.9
F_{1xf}/N	32.1	83.9	138.1	188.6	234.2	274.8	311.5	343.8

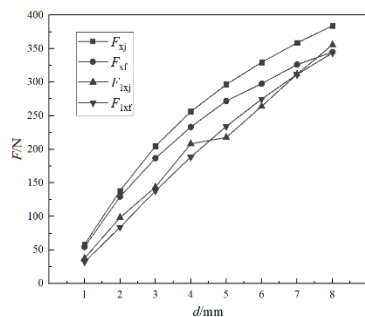


Figure 9: The change curve of the calculated value and the simulated value of the model 2

5. Conclusion

In this paper, an analytical model of axial magnetic force composed of rectangular cross-section permanent magnet ring is established based on the specific working conditions of well submersible pump. The relationship between axial bearing capacity of permanent magnet bearing and axial displacement, axial length of magnetic ring and radial thickness of magnetic ring is analyzed. The simulation results show that:

1) The calculation results of the model are basically consistent with the finite element simulation results. The error mainly comes from the magnetic flux leakage of the permanent magnet and the setting of the solution domain during the simulation.

2) The restoring force generated by the rotating magnetized permanent magnet bearing in the axial direction is greater than the sum of the axial magnetic force generated by the reverse magnetized permanent magnet bearing composed of these magnetic rings.

3) The axial length and radial thickness of the magnetic ring should be equal or close. When the thickness and width are equal, the magnetic energy of the permanent magnet bearing is in an ideal state.

References

- [1] Lin Wenhua, Mao Zhongyu, Li Xiangyang, et al. Analysis and Improvement of Axial Force Characteristics of Water Pump Turbine Pump Working Conditions [J], *Transactions of the Chinese Society for Agricultural Machinery*, 2020, 51(6): 133-137.
- [2] Wang Shuanghua, Study on Dynamic Pressure Lubrication Characteristics of Water-lubricated Thrust Bearings and Optimization of their Heterogeneous Surfaces [D], WU Han: Wuhan University of Science and Technology, 2019.
- [3] Wang Kai, Li Yu, Liu Houlin, et al. Numerical Study on Hydrodynamic Noise of Multistage Centrifugal Pump under Multiple Working Conditions [J]. *Vibration and Shock*, 2018, 37(9): 50-55.
- [4] Wei Yingsan, Shen Yang, Jin Shuanbao, et al. Scattering Effect of Submarine Hull on Propeller non-cavitation Noise[J]. *Journal of Sound and Vibration*, 2016, 370:319-335.
- [5] Wang Songlin, Tan Lei, Wang Yuchuan. Transient Cavitation Flow and Pressure Pulsation Characteristics of Centrifugal Pump [J]. *Vibration and Shock*, 2013, 32(22):168-173.
- [6] Zhang L, Wu H C, Li P, et al. Design, Analysis, and Experiment of Multiring Permanent Magnet Bearings by Means of Equally Distributed Sequences based Monte Carlo method[J]. *Mathematical Problems in Engineering*, 2019, 2019: 4265698.
- [7] Zhang Haibo, Qiu Yujiang, Jiang Shuyun. Analysis of the Equivalent Surface Current Model for the Permanent Magnet Bearing by Using the Integral Definition [J]. *Journal of Mechanical Engineering*, 2016, 52(7): 54-59.
- [8] Marinescu M, Marinescu N. A New Improved Method for Computation of Radial Stiffness of Permanent Magnet Bearings [J]. *IEEE Transactions on Magnetics*, 1994, 30(5): 3491-3494.
- [9] Fang J C, Le Y, Sun J J, et al. Analysis and Design of Passive Magnetic Bearing and Damping System for High-speed Compressor[J]. *IEEE Transactions on Magnetics*, 2012, 48(9): 2528-2537.
- [10] Zhang Jian, Sun Yuzhuo, Zhang Hailong, et al. Research on Magnetic Force Characteristics of Thrust Permanent Magnetic Bearing Based on ANSYS [J]. *Bearing*, 2014(4): 5-9.
- [11] Ohji T, Ichivama S. New Conveyor System Based on a Passive Magnetic Levitation Unit Having Repulsive-type Magnetic Bearings. *Journal of Magnetism and Magnetic Materials*[J], 2004, 272-276
- [12] Ohji T, Mukhopadhyay T, Iwahara M. Performance of Repulsive Type Magnetic Bearing System under Non-uniform Magnetization of Permanent Magnet. *IEEE Transactions on Magnetics*[J], 2000, 36(5), 3696~3698
- [13] Brad Paden. Design Formulas for Permanent Magnet Bearings, ASME. *Journal of Mechanical Design* [J], 2003, 125:734~738
- [14] Tian Lulin, Li Yan, Yang Guoqing, et al. Study of the Axial Magnetic Force of Radial Magnetization Bi-barrel-shaped Permanent Magnetic Bearings (PMB) [J]. *Mechanical Science and Technology for Aerospace Engineering*, 2007, 26(9): 1216-1219.
- [15] Tian Lulin, Li Yan, Tian Qi, et al. Axial Magnetic Force Analytical Model for Radial Magnetization Multi-annular Nesting Permanent Magnetic Bearings [J]. *Chinese Journal of Computational Mechanics*, 2010(2): 379-384.
- [16] Tian Lulin, Li Peng. Magnetic Analysis Model of Tapered Permanent Magnet Bearings [J]. *Chinese Mechanical Engineering*, 2014, 25(3): 327-332.